Computers and Electrical Engineering 103 (2022) 108386

Contents lists available at ScienceDirect

Computers and Electrical Engineering

journal homepage: www.elsevier.com/locate/compeleceng

Brain MRI analysis using deep neural network for medical of internet things applications☆

Momina Masood [a], Rabbia Maham [a], Ali Javed [a], Usman Tariq [b], Muhammad Attique Khan [c,*], Seifedine Kadry [d]

[a] Department of Computer Science, University of Engineering and Technology, Taxila 47050, Pakistan
[b] Department of Management Information Systems, CoBA, Prince Sattam Bin Abdulaziz University, Al Kharaj, Saudi Arabia
[c] Department of Computer Science, HITEC University, Taxila, Pakistan
[d] Department of Applied Data Science, Noroff University College, Kristinasand, Norway

ARTICLE INFO

Keywords:
Brain tumor detection
Deep learning
CenterNet
Keypoint estimation
Classification
IoT

ABSTRACT

Researchers are increasingly interested in leveraging the Internet of Things in medical and healthcare systems to provide better solutions such as remote health monitoring, personal fitness, and chronic disease management. A brain tumor is a potentially fatal cancer caused by the uncontrollable growth of brain cells that affects human blood cells and nerves. However, accurate classification of brain tumors is difficult due to the vastly different anatomical structures of healthy and tumorous tissues. We propose a framework for brain tumor localization and classification based on CenterNet. The proposed method uses the ResNet34 model with an attention block as a base network, which improves feature representation capacity by focusing on tumor locations and aids in tumor classification, particularly for a small tumor. Our method achieves 98.98% accuracy overall. Both qualitative and quantitative analysis demonstrated the efficacy of our approach for accurate detection and classification of the brain tumor than existing latest approaches.

1. Introduction

The Internet of Things (IoT) connects everyday physical things to the internet so that information can be transmitted or received between them. The concept of IoT has evolved from various underlying technologies such as sensors, embedded systems, and real-time data analytics. The IoT has made it possible to implement ambient assisted living through a variety of digital applications such as smart homes and cities, smart health monitoring, intelligent transportation, etc [1]. Timely and reliable health care has always been one of the highest priorities throughout human history. In the present day, personal mobile devices or wearables are becoming a more popular way of gathering personal data and interacting with physicians. The IoT offers a strong foundation for mobile health, which promotes person-centered care. The adoption of IoT in the medical industry has created various opportunities to design and build extremely sophisticated apps to address a wide range of complex human health issues [2].

The Internet of Medical Things (IoMT) concept has combined two domains namely IoT and healthcare [1]. IoMT is the network of medical devices and apps that can exchange data with healthcare information technology systems. The IoMT and cloud computing

☆ This paper is for special section VSI-aihc. Reviews were processed by Guest Editor Dr. Deepak Gupta and recommended for publication.

* Corresponding author.
E-mail address: attique.khan@hitecuni.edu.pk (M.A. Khan).

https://doi.org/10.1016/j.compeleceng.2022.108386
Received 10 December 2021; Received in revised form 2 September 2022; Accepted 6 September 2022
Available online 13 September 2022

offer remote monitoring of the patients and various decision support systems to doctors and caretakers. To minimize the mortality rate, it is critical to accurately identify and classify brain tumors at an early stage utilizing IoT technologies. The brain tumor is a deadly disease triggered by the irregular growth of brain tissue. According to the National Brain Tumor Society, around 700,000 persons in the US have a brain tumor, with an additional 85,000 expected to be diagnosed in 2021 [3]. Similarly, Cancer Research Corporation in the UK mentioned that over 42,000 patients having primary brain tumors lose life yearly. Brain tumors are grouped into 2 types: primary tumors and secondary tumors. Primary tumors are found in brain tissue, whereas secondary cancers spread from other areas of the human body to brain tissue through the bloodstream. Glioma and meningioma are deadly types of primary brain tumors that can may cause loss of a patient's life if not detected timely [4].

With such a large number of patients worldwide, several scanning approaches such as magnetic resonance imaging (MRI), Computed Tomography (CT), Magnetoencephalography (MEG), Positron Emission Tomography (PET), and X-ray are utilized for diagnostic purposes. MRI is the most widespread and harmless imaging technology employed in clinical practice since it does not involve any harmful ionizing radiation [5]. In addition, MRI scans have a high resolution and contrast between soft tissues, providing important details regarding tumor type, position, size, and shape in different formats. Typically, a professional radiologist manually annotates the tumor location from MRI images based on anatomical and physiological expertise. Unfortunately, this manual inspection procedure is time-consuming, laborious, and even prone to mistakes due to the influx of patients. Hence, an early tumor diagnosis and accurate categorization is necessary as it can help in the treatment and increase the survival rate of patients.

In recent years, due to advancements in technology, automatic Computer-Aided Diagnosis (CAD) and expert systems are being developed to alleviate the workload of radiologists and doctors. These systems perform automated diagnosis and classification of tumors that provide insight to healthcare professionals in making therapy-related decisions. However, automated tumor identification is still difficult due to considerable inter and intra-shape, texture, and contrast variations [6]. Additionally, the tumor can occur anywhere in the brain, and its boundary is frequently blurred by healthy brain tissue. Furthermore, the existence of MRI abnormalities such as noise and distortion introduced by imaging systems or acquisition procedures makes accurate tumor delineation more difficult.

Numerous Machine Learning (ML) and Deep Learning (DL)-based techniques are employed to develop a highly accurate and robust CAD system for automatic identification and categorization of brain tumors. The ML-based methods include Support Vector Machines (SVM), K-Nearest Neighbors (KNN), and Principal Component Analysis (PCA). These approaches are easier to deploy and do not use a huge amount of training datasets. However, the performance is limited due to hand-craft features as employing a large feature set increases computational complexity, whereas using a limited feature set reduces identification performance. Thus, the detection effectiveness of these approaches relies on the nature of extracted features [3].

Recent studies have proven the efficacy of DL-based techniques in a range of fields, including medical domain. Meanwhile, IoMT technology is also emerging in the healthcare sector for gathering data and delivering more efficient services to patients. The DL extracts meaningful features automatically from collected data, resulting in considerably improved performance. The Convolutional Neural Network (CNN) is the most popular DL model that has demonstrated effective pattern recognition performance due to its weight-sharing nature. Popular image classification models such as AlexNet, GoogleNet, VggNet, ResNet, DenseNet, and different variants are extensively employed in existing brain tumor classification systems. These approaches perform classification without providing information about tumor location and have a high false-positive rate. Recently, object detection-based DL algorithms are adopted for the detection of brain tumors to attain maximum sensitivity (recall rate). These methods determine the precise location and class of the tumor, however, rely primarily on a predetermined set of anchor boxes i.e., scale and aspect ratio, with each anchor box sampled evenly across spatial locations. Thus, these approaches introduce excessively many hyper-parameter choices during training and are computationally expensive.

Despite recent advances, DL methods for brain tumor detection and classification still need to be improved in terms of robustness and accuracy. In addition, computationally efficient models with fewer training parameters and faster training speed without compromising performance are required. In this work, we introduced a computationally efficient method based on the CenterNet model [7] to detect and classify brain tumors from the input MRI images. We employed CenterNet for brain tumor detection because it has recently demonstrated good performance in real-time target recognition and classification. Instead of using sliding anchors that compute features by identifying bounding boxes, the CenterNet uses a center keypoint for the prediction of both the tumor class and bounding box at the same time, thus it is faster and computationally efficient. In our work, we customized the backbone network by employing an additional lightweight attention module [8] with ResNet [9]. Our improved backbone network helps the CNN network to focus on the tumor locations, thus improving the detection accuracy and achieving high sensitivity.

The main contributions of our work are:

1 We proposed an improved CenterNet-based architecture that can precisely localize and categorize brain tumors from MRI images by representing them in a much simpler manner i.e., as a central point.
2 We presented ResNet34 as the backbone of CenterNet along with an attention block for feature extraction to improve the accuracy of localization and classification of brain tumors.
3 We presented a computationally efficient brain tumor detection technique that does not use the anchor-boxes approach and decreases the number of hyper-parameters that are required to be tuned heuristically to achieve high performance.
4 Extensive experiments are performed to show the efficacy of the proposed method, which outperforms existing brain tumor classification methods in terms of robustness and accuracy.

The rest of our work is structured as follows: Section 2 defines the overview of existing literature, and Section 3 presents a detailed explanation of the proposed method. Section 4 discusses the datasets used, the evaluation settings employed, and the experimental

results obtained. Section 5 reports the conclusion of our work.

2. Related work

Recently the IoMT has become more prevalent in healthcare systems, allowing patients with serious illnesses and at-risk groups such as older citizens to be monitored in real-time [1]. Brain tumors are regarded as the most serious illness because of life-threatening issues. Different studies are conducted on DL applications for IoT to provide e-healthcare services. Study [2] reviewed different aspects of IoT-based techniques in the healthcare field and proposed various medical network designs and technologies that serve as the foundation for IoT available and help in the transfer and collection of data in medicine. Various types of medical images have been used for the detection of brain abnormalities such as CT scan, MEG, MRI, PET scan, etc. In [10], six CNN models have been implemented for

Table 1
Summary of existing techniques for the brain tumor detection.

Sr. No.	Ref.	Type	Dataset	Algorithm	Results	Advantages	Issues	Features Extracted	Tool
1	[20]	Classification into 3 types	3 different data sources	Ensemble approach	98.96 accuracy	This method has improved generalization.	The method is computationally complex	Pre-trained models VGG19, Xception, EfficientNet, ResNet50, and Inception-V3	Python
2	[4]	Classification and Segmentation	Figshare dataset (3064 images), private images (600)	CNN model with superpixel technique for segmentation	98.54 accuracy, 97.40 precision, 98.63 sensitivity, and 98.63 specificity	This method is effective at extracting complex characteristics.	Low detection performance for small-size tumors	Darknet model	Matlab
3	[21]	Classification into 3 types	BRATS and Figshare dataset	Block-wise model fine-tuning with KNN classifier	98.69% accuracy	This approach can effectively identify small-sized tumors due to block-wise fine tuning	Lacking detailed experimental results	VGG19	-
4	[22]	Classification into 2 types	Kaggle and TCIA	CNN	98% accuracy	This method is less computationally complex	Lack of robustness analysis of the model	CNN	Python
5	[23]	Classification into 3 types	Figshare dataset (3064 images)	CNN with global average pooling	95% accuracy	This method is less prone to overfitting and effective at extracting complex characteristics.	Needs performance improvement	ResNet34	Python
6	[24]	Classification and Segmentation	BRATS (2013, 2014, 2015, 2016, 2017, 2018), ISLES 2018	Ensemble approach	The lowest accuracy is 96.67% on BRATS-2013, highest accuracy is 98.91% on BRATS 2015	This method can accurately delineate tumor borders independent of heterogeneity.	The method requires extensive preprocessing and utilized an axial view of brain slices only	Pretrained AlexNet, and GoogleNet	Matlab
7	[25]	Detection	BRATS 2017	CNN	84.19%	This method is effective at extracting complex characteristics.	No clear information on the datasets, no clear method, and no comparison with existing techniques.	ImageNet database	Python
8	[26]	Classification into 3 types	Figshare dataset (3064 images)	AlexNet, VGGnet and Googlenet	VGG16 attained an accuracy of 98.69%	This approach does not require pre-processing.	No comparison with existing techniques, not as detailed related work and results	CNN for feature extraction	Caffee library 7
9	[27]	Classification and Grading	Figshare by cheng and Rembrandt (3064 and 516)	CNN for classification and grading	96% and 98% accuracy	It is a computationally efficient approach.	High learning rate and complex architecture based on 16 layers	CNN	Matlab 2018b plus python

the classification of brain tumors. These models had a different number of layers, while two CNN models had dropout layers for the regularization. In addition, stopping criteria along with batch normalization was also used by two CNN models. The last two models were used without these layers. One of the model yield the best accuracy of 96%.

DL algorithms play a vital role in image and pattern recognition applications [11]. New architectures have been implemented using complex structures to detect and recognize diseases through images. In [12], data pre-processing has been used for the significant efficiency of the CNN-based model for the categorization of brain tumors. Patch extraction and rotation have been employed as traditional data augmentation methods on the 3064 images. Furthermore, images were resized to 28×28 for the reduction of the algorithm's complexity. In the end, capsule-net was used for the brain tumor classification trained on three classes such as glioma, pituitary, and meningioma tumor. The result showed significant performance due to pre-processing. A binary brain tumor classification model has been proposed using MRI images [5]. They employed AlexNet and VGG16 to extract the features. They used the hypercolumn technique to enhance the features and fused the features with both models. Moreover, they employed a SVM to categorize the images and gave 96% accuracy. In [13], DL and statistical technique have been used to differentiate the tumor and non-tumor images. They employed information-theoretic measures, scattering transforms and wavelet packet tallis entropy to extract the features from images. Moreover, deep autoencoders based algorithm and softmax function has been used for the classification. They have attained 98.5% accuracy. In [14], ResNet50 has been utilized for the binary categorization of brain tumor images. The architecture was modified using 8 additional layers to the original architecture. Furthermore, they used the MRI dataset attained from Kaggle. The algorithm was compared with Googlenet, Alexnet, Densenet, etc, and showed 97% accuracy. A novel architecture named BrainMRNet CNN has been proposed by [15]. The model was composed of three phases i.e. convolution block attention for the learning of channel and spatial information, residual block for learning of important features, and hypercolumn technique. The classification results showed an accuracy of 96.05%. The generative adversarial networks based technique has been proposed in [16]. Moreover, data augmentation was used to produce more naturalistic data of MRI images. For the last layer, they used the softmax function for the classification attaining 88% accuracy. In [17], the authors used a transfer learning strategy to evaluate the performance of various CNN models such as VGG16, Inception-V3, and ResNet50 for the classification of brain tumors. The results showed that the Resnet50 model reaches the highest accuracy of 95% among other models. In [18], the authors designed a lightweight CNN model comprising five layers for the extraction of deep features from input MRI images. Then, an SVM classifier is trained to classify the extracted features. This method attained an accuracy of 95.82% for multi-class brain image classification. Another work in [19] suggested a deep CNN architecture having 13 convolutional layers for brain MRI image classification. The method achieved an overall classification accuracy of 97.2%. Aurna et al. [20] presented an ensemble approach using pre-trained CNN models such as VGG19, ResNet50, inceptionV3, etc. Initially, the deep features are extracted and then the features of top-performing models are concatenated using a two-stage strategy. To further eliminate the interrelated features, the PCA algorithm is applied to select the important features. This approach shows improved classification performance, however, at the expense of increased computation and relies on extensive experiment and selection choices. In [4], the authors employed DarkNet-19 and DarkNet-53 model for the localization and classification of brain tumor into multiple class. To further obtain the precise tumor region, a super-pixel technique is used to segment the localized tumor. Different wavelet and geometrical augmentation are also applied to increase the diversity of training samples and improve the generalization performance. The method obtained an overall accuracy of 98.54% on samples from the T1W-CE MRI dataset.

In [21], a transfer learning-based algorithm has been proposed for small dataset problems. They used pre-trained VGGnet which performed block-wise tuning for the 6 blocks. Furthermore, for individual blocks there exist a different number of layers. The algorithm attained 97.28% and 98.69% accuracy for the datasets BRATS and CE-MRI. In [22], a novel brain tumor classification system based on CNN using MRI imaging has been proposed. They used two datasets such as Kaggle and TCIA and evaluated their algorithm using three optimizers. The RMSprop showed the best results giving an accuracy of 98%. The ResNet34-based architecture has been proposed in [23] named G-RESNET. The flattened layer was replaced with a max-pooling layer and a new loss function was utilized. In the end, feature fusion was performed using low and high-level features. The proposed algorithm attained 95% accuracy. In [24], a novel method for the detection and classification of tumors into two classes such as malignant and benign has been developed. The score level fusion for output vectors was computed using pre-trained networks i.e. AlexNet and GoogleNet for the classification. They used the BRATS dataset to classify into low and high grades. They also compared the time duration of training and testing and curves for loss functions with existing techniques. Summarized details of existing techniques have been presented in Table 1.

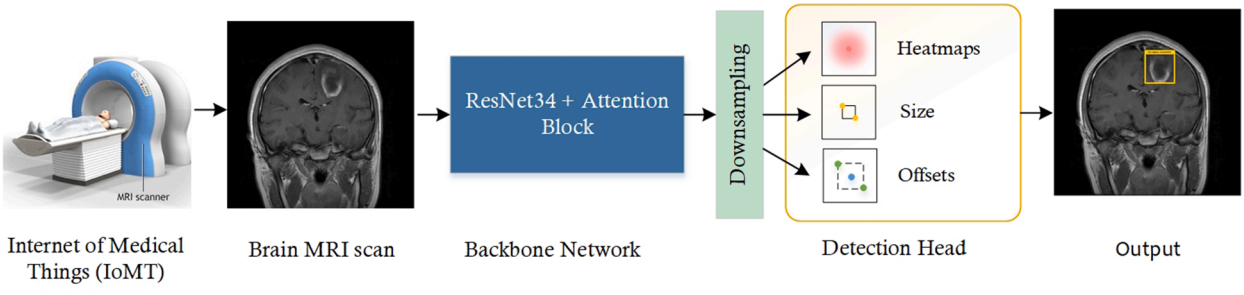

Fig. 1. The overall architecture of the proposed model for brain tumor detection and classification using the improved CenterNet model.

3. Proposed method

This section presents the proposed methodology adopted for the classification of brain tumors. For an input MR image, the ultimate aim is to automatically identify and determine the class of tumor i.e., glioma, meningioma, and pituitary. Fig. 1 shows the overall architecture of the proposed method. Initially, MRI scans of the patients are collected, which are fed to the proposed CNN model that is built using the CenterNet network [7]. In our work, we improved the CenterNet architecture by employing ResNet34 with convolution attention block [8] as the feature extraction network. Based on computed features, the detection head performs localization and categorization of the tumor using center locations.

3.1. CenterNet model

The proposed model is based on an anchor-free, one-stage detector namely CenterNet [7]. The CenterNet model uses keypoint estimation for the identification of an object. Initially, the model locates the center point of the potential tumor region and then uses image features from that center position to regress the size of the identified tumor. In this work, we have improved the CenterNet model for the detection and classification of brain tumors. We simplified the backbone network to increase model effectiveness and achieve more accurate results. The improved backbone computes high-level discriminative information that improves detection accuracy.

The motivation for employing the CenterNet model for the identification of brain tumors is its ability to effectively identify small objects, high execution speed, and computational efficiency as compared to previous models. The one-stage detector-based approach [28] uses a large number of predefined anchor boxes for detecting an object of different sizes. This results in high false-positive predictions due to redundant anchor boxes. Moreover, it introduces an excessive amount of hyper-parameter choices i.e., the number of anchors, scale, and aspect ratios that are required to be adjusted depending on the problem which increases training complexity. The two-stage detector-based method [3,29] use two separate networks for identification and classification. Initially, an RPN is used for the generation of candidate regions and then a separate network is used for the regression and classification of each proposed region. Therefore, these methods are computationally expensive and are not robust for real-time prediction. The CenterNet model addresses the limitation of existing one-stage and two-stage detectors by employing a center keypoint prediction mechanism that is computationally efficient. The CenterNet model is proven to function more simply and efficiently by predicting both key points and bounding boxes of objects in an image at the same time. Instead of using anchor bounding boxes, the model assesses the tumor as single points by estimating the x and y coordinates of the tumor's center as well as its region of coverage (height and width), which improves accuracy and speed by reducing the number of detected wrong bounding boxes. These properties make it suitable for real-time illness diagnosis in clinical practice.

The overall architecture of the CenterNet model comprises of two major components; the backbone network and the detection head (Fig. 1). Our backbone network is based on a highly efficient feature extractor the ResNet model that captures robust and highly discriminative semantic features from the input image. In addition, we added a convolutional attention block to focus on tumor locations, which facilitates the following detection task. The detection head predicts the center location of tumors along with the size i.e., the width and height of bounding boxes corresponding to each center. Moreover, to obtain accurate center locations, offsets to the x and y axes are computed using the detection head, which is then used to fine-tune the placement of individual center locations.

3.1.1. Backbone network

A backbone network extracts visual features which provide a semantic and robust representation of an image. The baseline CenterNet can be run with a variety of backbones [7]. The original CenterNet employs Hourglass and HRNet as the backbone. Although these backbones have improved detection accuracy, however, these models are relatively large due to the huge number of parameters and computationally complex that directly affect the speed and overall efficiency of the model. Moreover, the accuracy of the feature

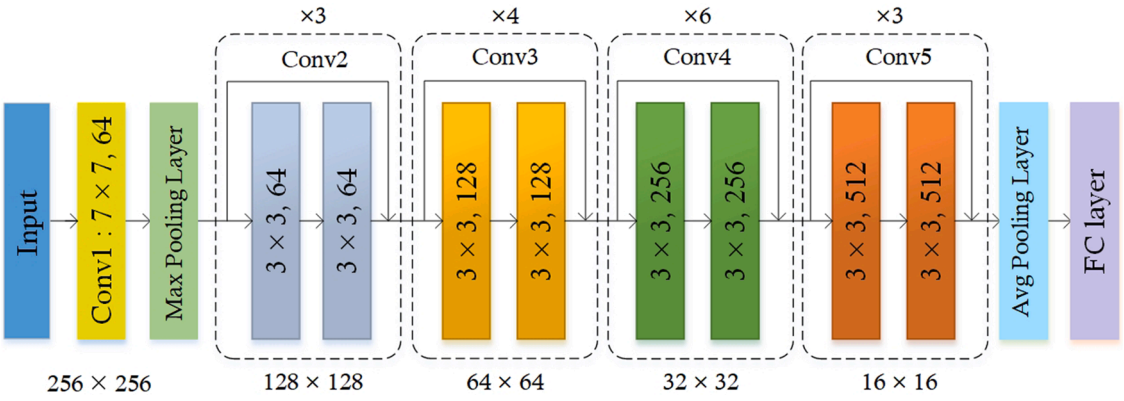

Fig. 2. Network architecture of the ResNet34 model.

extractor impacts the detection accuracy. In this work, we have used ResNet34 with Convolutional Block Attention Module (CBAM) as the backbone of our detection model to extract richer and more abstract features from the input image. We employed Resnet34 because its performance-to-accuracy trade-off is appropriate for the problem (i.e., there are just three classes: glioma, meningioma, and pituitary tumor). Since the model is small and it has low computational complexity.

The ResNet model [9] is a state-of-the-art classification network that uses residual mapping and identity shortcut connections between layers. The identity shortcut connections allow reusing the preceding feature maps that lead to better results and easier training as compared to other deep networks. The motivation to apply the ResNet model is its simple design strategy and improved feature representation with depth. Typically, in deeper networks, the performance degrades due to the gradient vanishing with the increase in depth of the network. To alleviate this issue, shortcut connections are added to the deep neural networks which bypass one or more layers and constitute the building block of the ResNet. Fig. 2 shows the architecture of the ResNet34 model comprising 34 layers and 4 convolutional (Conv) stages. Each stage consists of multiple residual blocks stacked one over the other comprising 3×3 convolutions. In the convolutional layer, the convolutional filter convolves an image with kernels to extract a specific keypoint representation map of the input. The output y^j of the convolutional layer is computed as follows:

$$y^j = f\left(y^{j-1} \times w_i^j + b_i^j\right) \tag{1}$$

where y^{j-1} denotes the keypoint representation map of the convolution kernel in the (j-1)th layer, w_i^j and b_i^j shows the weight and bias of the learnable ith convolutional kernel in the jth input layer and the f denotes the activation method. The stacked layers in residual networks execute a residual mapping by forming shortcut connections that perform identity mapping (x). Their outputs were combined with the stacked layers' output residual function $F(x)$ and can be expressed as follows:

$$H_j(x) = F_j(x) + x \tag{2}$$

where x is the input, and F represents the series of the convolutional operations for the jth residual block.

Attention module: Based on the properties of brain MR images, the larger portion comprises of non-useful background areas. An attention block is added to the feature extraction network to assist the network to focus on the location containing the tumor. The attention mechanism enables the network to selectively concentrate on important information such as the tumor region while suppressing the irrelevant things, such as the background region to enhance the detection accuracy. In our proposed model, we employed the CBAM module as the attention block. The reason for using CBAM block [8] is because of its lightweight architecture, which offers negligible overheads and can be trained end-to-end along with base CNNs. The studies also showed that using the CBAM attention mechanism assists the model in selecting intermediate features more effectively. Fig. 3 shows the structure of the attention block. The CBAM refines the CNN extracted features by combining spatial and channel-wise attention, which improves the performance of DNN. The Channel attention module seeks to adaptively adjust channel-wise feature responses, whereas the spatial attention module emphasizes the use of focusing on ROIs.

The input features are initially processed by the convolution layer, as introduced in Eq. (1). For an intermediate keypoint representation map G, the CBAM block sequentially infers the spatial A_s and the channel A_c attention maps. In the channel attention module, initially, the input keypoint representations map are parallelly processed by an average pooling (AvP) and maximum pooling (MaP) layer and then passed to a shared multi-layer perceptron (MLP) with one hidden layer. Finally, an element-wise summation operation is used to combine the output keypoint representation. The A_c is computed as:

$$\begin{aligned} A_c(G) &= \sigma(\mathrm{MLP}\ (\mathrm{AvP}(\mathrm{G})) + \ \mathrm{MLP}\ (\mathrm{MaP}(\mathrm{G}))) \\ &= \sigma\left(\mathrm{X}_1\left(\mathrm{X}_0\left(G^c_{max}\right)\right) + \ \mathrm{X}_1\left(\mathrm{X}_0\left(G^c_{avg}\right)\right)\right) \end{aligned} \tag{3}$$

Where σ shows the sigmoid activation method, the X_1,$X_0$are learning weights, G^c_{max} and G^c_{avg} are generated intermediate keypoint maps.

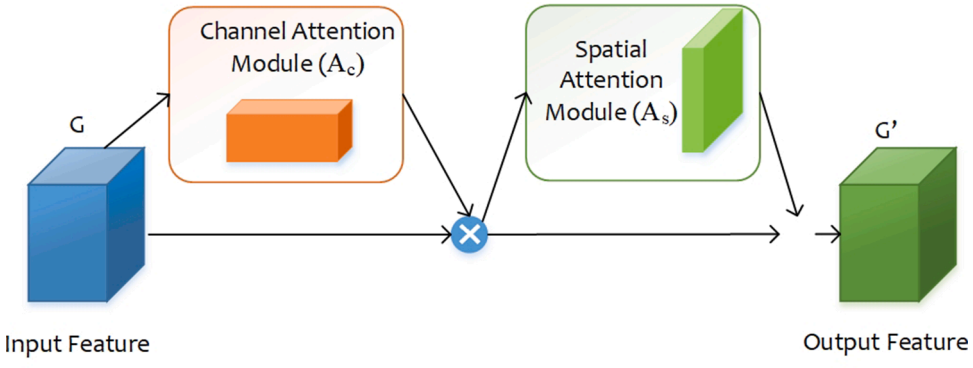

Fig. 3. The structure of the CBAM module.

Similarly, the A_s is computed by applying AvP and MaP operation serially along with the channel axis and output is passed to the convolution layer that is followed by the sigmoid activation method. The A_s can be expressed as:

$$A_s(G) = \sigma\left(f^{7\times7}(\mathrm{AvP(G)};\mathrm{MaP(G)})\right) \tag{4}$$

Where f denotes the convolutional operation with a kernel of the size 7×7.

Fig. 4 shows the architecture of the improved backbone based on the ResNet34 and CBAM block. We have added a 7×7 Attention module after Conv1. The introduced module assists the network in focusing on tumor locations and extracting more critical information from the image and thus improving the identification accuracy of tumors. As described in [28], the downsampling step in the first convolutional layer may degrade model performance, particularly for very small-sized tumors. To deal with such a situation, we have modified the early layers in the original ResNet34 model. We replaced the initial 7×7 convolutional layer and max-pooling layer with three stacked 3×3 convolutional layers. Additionally, to reduce the computational cost, the channel is set to 64 for newly added convolution layers.

3.1.2. Detection head

The feature map obtained from the backbone head is fed to the detection network that comprises of three convolutional branches; a heatmap branch, a size branch, and an offset branch; where each of these produces a corresponding part of detection [7]. The detection head detects the tumor by estimating corresponding center locations using a heatmap. The other relevant properties such as tumor size are predicted using image features from the central location. Furthermore, the detection head also computes offset to adjust the location of the center point to obtain a more precise center position. Initially, the extracted feature maps are down-sampled by using a convolutional layer with stride $D = 2$. The features are then passed to the network's heatmap, size, and offset branches, with each branch producing the respective part of the detection, as explained below.

The heatmap head computes the likeliness of the center location of the tumor over the down-sampled deep features to localize the tumor region together with the respective class. Let keypoint k is any center point, it can be placed on a groundtruth heatmap using a Gaussian kernel defined as:

$$\mathrm{H}_{xyc} = \exp\left(-\frac{(x-\hat{k}_x)^2 + (y-\hat{k}_y)^2}{2\sigma_k^2}\right) \tag{5}$$

where x and y represent actual groundtruth keypoint coordinates in the heatmap, $\hat{k}_x$ and $\hat{k}_y$ indicate the corresponding locations of the predicted keypoint in the low-resolution heatmap. σ_x is the size adaptive standard deviation that is adjusted automatically according to tumor size as described in [7]. The H_{xyc} denotes the center of a potential keypoint of detected category c; a value of one indicates the presence of a tumor at the current position; otherwise, it represents the background.

The dimension head is responsible for determining the size of the tumor. Using the features at the center (positive point), it predicts the coordinates of the bounding box. The dimension of the bounding box for a candidate tumor k having coordinates (x^i_{max}, x^i_{min}, y^i_{max}, y^i_{max}) can be estimated through the L1-Norm loss which is $s_i = (x^i_{max} - x^i_{min}, y^i_{max} - y^i_{min})$

The offset head is calculated to decrease the quantization error caused by downsampling of the input sample that may result in some precision loss, reducing the accuracy of the predicted center position, particularly for small tumors. Thus, to adjust the corner locations, the position offsets are calculated for each center point.

3.2. Loss function

The multi-loss function of the CenterNet model combines the loss of center point prediction (healthy/affected region), the loss of offset (position), and the loss of bounding box (size). The performance of the model is assessed by combining these three different losses. The center loss is intended to allow the model to learn aspects of increased weight over time to focus on the affected areas. Then,

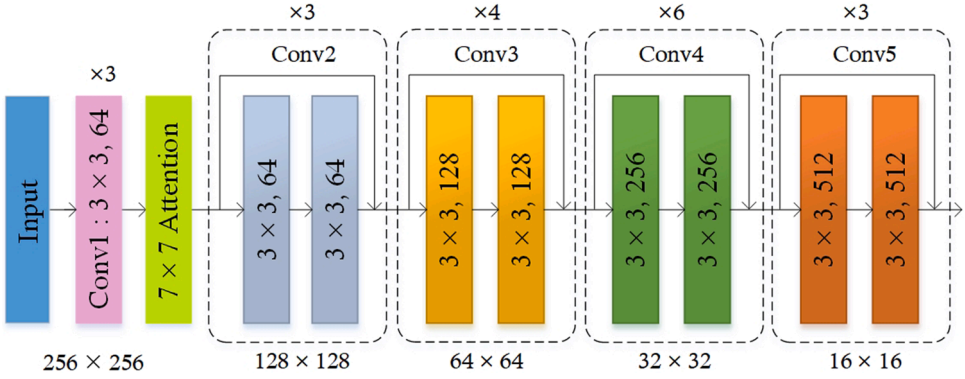

Fig. 4. Improved architecture of feature extraction network with attention block.

the loss of location and offset to the center point are utilized to determine the exact size, orientation, and position. The advantage of employing the multi-loss method is that it assists the model in learning to distinguish between the actual and predicted values throughout the training phase, and allows it to precisely localize the affected region with the relevant class. The overall training objective L_{total} is the summation of three different losses, given as follows:

$$L_{total} = L_{heat} + \lambda_{size} L_{size} + \lambda_{off} L_{off} \tag{6}$$

where L_{total} denotes the complete detection loss function used in CenterNet. The L_{heat} is heatmap, L_{size} is dimension loss responsible for computation of bounding-box and L_{off} is the smooth L1 loss responsible for offset correction. The parameter λ_{size} and λ_{off} are constants and set as 0.1 and 1 respectively.

The L_{heat} is a penalty-reduced per-pixel logistic regression with a focal loss. The focal loss is a modified binary cross-entropy loss that gives an extra penalty to less confident predictions and is defined as:

$$L_{heat} = \frac{-1}{M} \sum_{xyc} \begin{cases} \left(1 - \widehat{H}_{xyc}\right)^{\varphi} \log\left(\widehat{H}_{xyc}\right) & \text{if } (H_{xyc}) = 1 \\ \left(1 - H_{xyc}\right)^{\omega} \left(\widehat{H}_{xyc}\right)^{\varphi} \log\left(1 - \widehat{H}_{xyc}\right) & \text{otherwise} \end{cases} \tag{7}$$

Here, M represents the total number of keypoints i.e., tumor in an image. $\widehat{H}_{xyc}$ and H_{xyc}represent the predicted and the respective groundtruth keypoint center. The φ and ω are the hyperparameters of focal loss that control the contribution of each point and are set as 2 and 4 respectively. The offset loss is an L1-Norm loss where all classes share the same offset prediction. The offset loss is defined as

$$L_{off} = \frac{1}{N} \sum_{t} \left| \widehat{O}_{\widehat{t}} - \left(\frac{t}{D} - \widehat{t}\right) \right| \tag{8}$$

Where $\widehat{t}$ is a predicted keypoint obtained from $\widehat{H}$, $\widehat{O}$ is predicted offset of keypoint $\widehat{t}, t$ is the corresponding true keypoint, and d is the scaling factor as defined above. The L_{dim} is calculated as:

$$L_{dim} = \frac{1}{n} \sum_{i=1}^{n} |\widehat{s}_i - s_i| \tag{9}$$

Here, $\widehat{s}_i$ is the predicted bounding box coordinates, while s_i is showing the actual dimensions of bounding boxes from groundtruths.

4. Experimental evaluation

In this study, we have proposed a pre-trained DL-based algorithm i.e. CenterNet with ResNet34 having attention block as a base network for the detection and classification of brain disease. The proposed framework was executed using Python on an Nvidia GTX1070 GPU-based system. In the proposed approach, we employed the framework using pre-trained weights attained from MS-COCO and implemented transfer learning to fine-tune the CenterNet model on our dataset for brain tumor detection and classification. The training parameters for the Custom CenterNet model are given in Table 2.

4.1. Dataset

For the performance evaluation, we used two datasets i.e. Figshare dataset and the open-source dataset from Kaggle. Figshare dataset consists of T1 contrast-enhanced MRI scans (2D) acquired from 233 patients to build 3064 images of scans. The dataset consisted of three classes representing brain tumor types such as meningioma (708), glioma (1426), and pituitary (930). The class distribution of the dataset consists of 23% for meningioma, 30% for pituitary, and 46.5% for glioma. These images were taken in the Nanfang Hospital of China. All the images are in greyscale form and have a dimension of 512 × 512. The sample images of brain tumors from the dataset are shown in Fig. 5. The summary of the Figshare dataset is given in Table 3. The second dataset of Kaggle consists of 255 T1 modality MRI scans. It has 98 images of a healthy brain and 155 images of a tumor. Therefore, for the evaluation of the proposed system over healthy images, we have used only healthy brain images from this dataset i.e. 98. Fig. 6 shows the sample images that are challenging in terms of tumor textural complexity, color variations, noise, position, varying acquisition angles, etc. All the images were of varying sizes therefore we resized them to 224 × 224 for using as input in our proposed framework.

Table 2
Training parameters for the proposed model.

Framework parameters	Value
Epochs	30
Learning rate	0.001
Batch size	8
Confidence score threshold	0.2
Unmatched Threshold	0.5

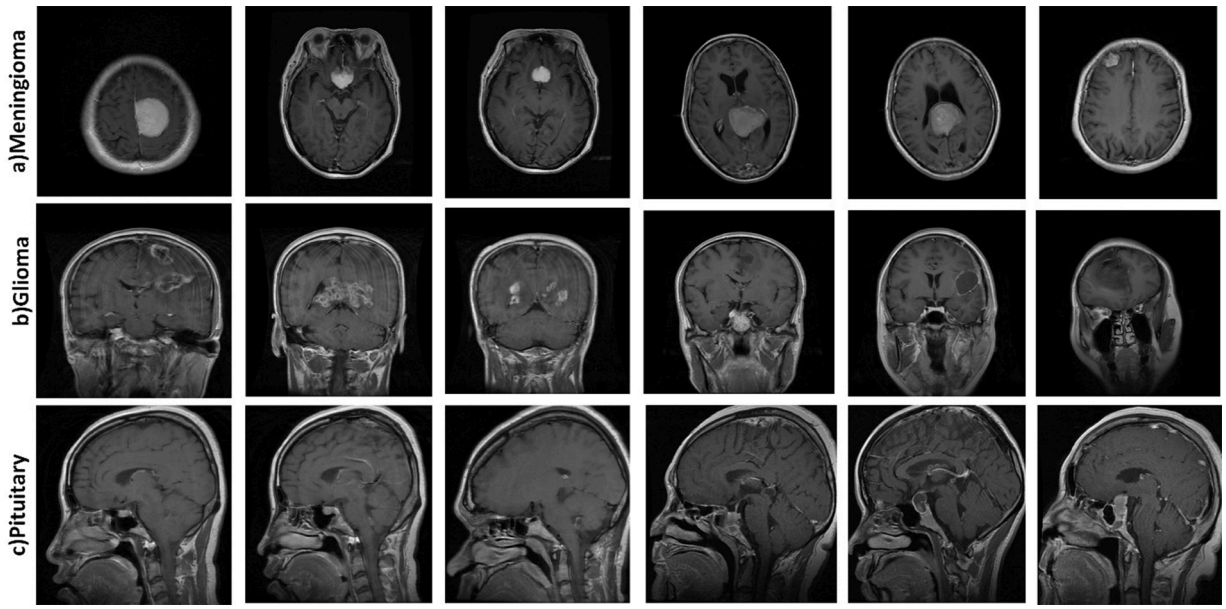

Fig. 5. Samples from figshare dataset.

Table 3
Summary of the figshare dataset.

Tumor Type	No.of Patients	MRI View	No. of Images	Total
Meningioma	82	Axial Sagittal Coronal	209 231 268	708
Pituitary	62	Axial Sagittal Coronal	291 320 319	766
Glioma	89	Axial Sagittal Coronal	494 495 437	1426
Total	**233**		**3064**	**3064**

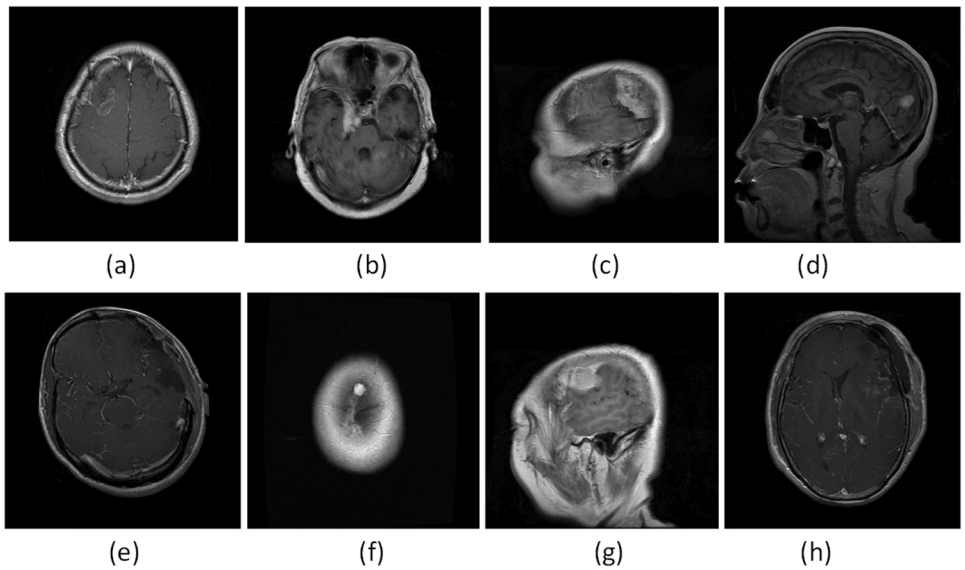

Fig. 6. Sample images having a tumor with different colors, positions, sizes, and various distortions. (a, b, d) textural similarity; (c) blurriness; (e, h) low contrast; (f) noisy sample; (g) brightness and blurry effect.

4.2. Evaluation metrics

For the evaluation of the proposed framework in terms of detection and classification, we utilized some standard metrics evaluation metrics i.e. accuracy, precision, recall, and F1 Score.

Accuracy: Accuracy is used to assess the overall performance of the proposed method on the data.

$$Accuracy = \frac{TP + TN}{TP + TN + FP + FN} \tag{10}$$

Where the true positive, TP, represents the number of images that were classified as correctly diseased class i.e. Meningioma, Pituitary, and Glioma. Whereas false positive, FP, represents the images classified incorrectly as diseased and in reality they are healthy. Moreover, false negative, FN, represents the frames that are classified as healthy and belong to the diseased class. False-positive, FP, are those images that are classified as diseased, and in reality, they belong to the healthy class.

Recall: Recall (R) has been computed referring to the percentage of images that were diseased and the system recalled them. The equation of recall is given below.

$$R = \frac{TP}{TP + FN} \times \ 100 \tag{11}$$

Precision: Precision (P) is computed referring to the percentage of images that are correctly classified using the proposed framework. The equations of Precision and F1 Score are given below:

$$P = \frac{TP}{TP + FP} \times \ 100 \tag{12}$$

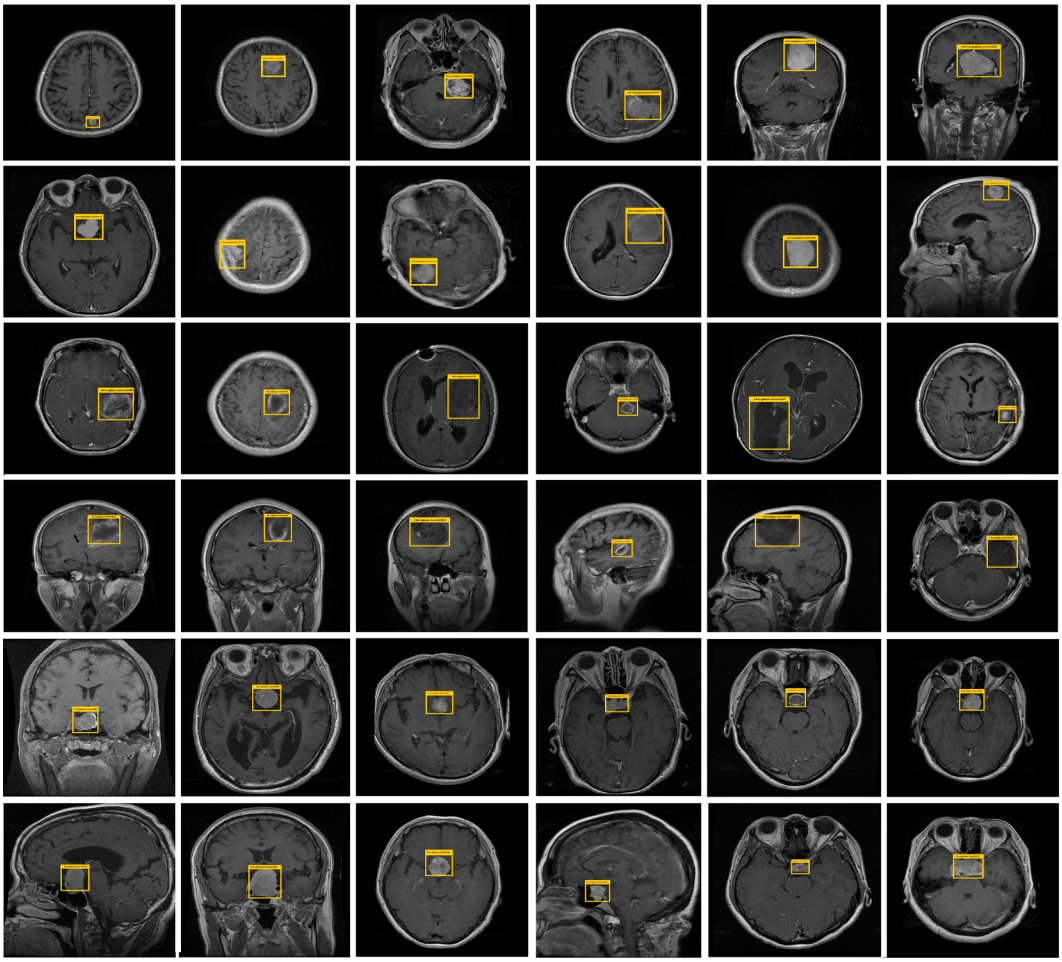

Fig. 7. Samples of the localized tumor by using the proposed method.

$$F1\_Score = \frac{P * R}{P + R} \times 2 \tag{13}$$

4.3. Performance evaluation of custom CenterNet

In this section, we discussed the analytical results of the proposed system. The accurate detection of the tumor cells in the brain is necessary to classify them using a computerized system. Therefore, we analyzed the localization performance of the CenterNet framework through experiment. We evaluated all the test samples of both datasets i.e. Figshare and Kaggle. The localization results of the proposed methodology are shown on image samples in Fig. 7. It can be estimated from the visual results that custom CenterNet with ResNet34 having attention block can detect and classify brain tumors accurately. We also evaluated the performance of CenterNet with ResNet34 without attention block, however, the results were not as significant as with attention block. In addition, the reported technique is robust to various image-related issues such as blurring, contrast, and distortions. The center keypoint estimation characteristic in CenterNet makes it able to effectively detect and localize the multiple tumor cells in the brain MRI images. Moreover, the proposed algorithm can deal with problems of change in location, size, and structure of tumor cells by accurately identifying them.

In addition, the performance evaluation of the proposed system with attention block over both datasets is shown in Fig. 8. The accuracy of our proposed framework with attention block is 98.97% over the Figshare dataset and 99% over the Kaggle dataset. While without attention block accuracy is 95% and 91%, respectively. The recall of our proposed framework is 99.92% and 99.1% over Figshare and Kaggle respectively. The precision of our proposed system is 99.52% for Figshare and 99.2% for the Kaggle dataset. The F1 score of the proposed system is 99.72% and 99.15% over Figshare and Kaggle datasets, respectively.

4.4. Cross-validation

Here, we discussed the performance of the proposed model using five-fold cross-validation. The most important challenge was to examine whether the model perform better on the test set even while it did so better on the training set. Hence, the issue of overfitting or underfitting is resolved at this stage using a validation set. In the first experiment, we split the dataset into 70% for training and 30% for validation. At the end of each iteration, the performance of the model is analyzed till the error of validation approaches reaches zero. In normal validation, there exist several issues such as usage of the same data in repetition, choosing a correct validation set, etc. Therefore, we employed the 5-fold cross-validation in which one subset is utilized for validation of the model against the trained model on four other sub-sets. The average loss for cross-validation attained was 0.0521 after the experiment was performed. The comparative results with existing techniques that performed five-fold cross-validation for brain tumor detection are shown in Table 4.

In Table 4, it can be seen that our proposed model without attention block attained 94% accuracy while with attention block outperforms the existing technique for five-fold cross-validation by achieving 97.23% accuracy. After our proposed algorithm the fine-tuning of VGG19 and VGG16 [6] attained 94.82% and 94.65% accuracy for cross-validation. All other algorithms attained less than 94% accuracy for the five-fold cross-validation.

4.5. Comparative analysis with other DL models

In this section, we have compared our proposed model (with attention block) with existing DL models for brain tumor detection. We performed the detailed experiment using 711 test images based on confusion matrix, accuracy, precision and recall, and F1 Score. A

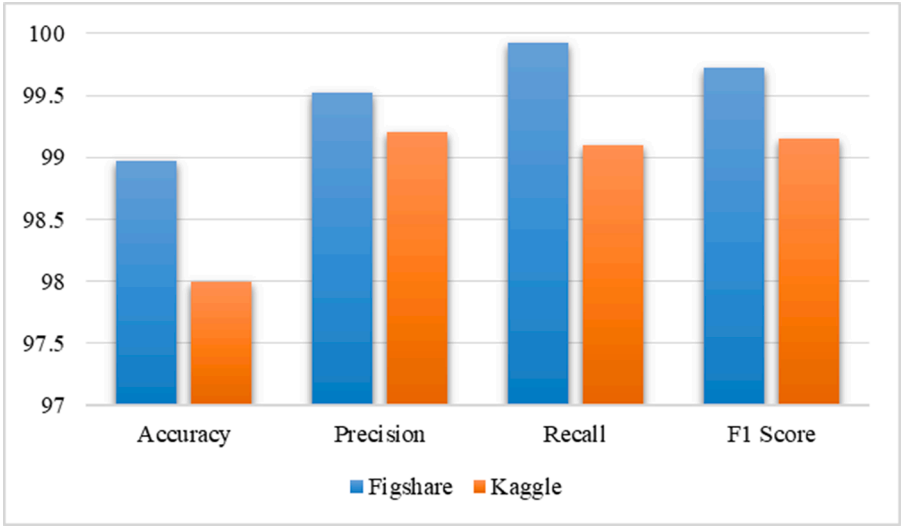

Fig. 8. The performance of the proposed system over both datasets.

Table 4
The comparison with existing techniques that used five-fold cross-validation.

Methodology	Accuracy (%)
CNN [25]	84.19
CNN + Fully connected NN [30]	91.43
Fine-tuning VGG16 [6]	94.65
Fine-tuning VGG19 [6]	94.82
The proposed model (without attention)	**94**
The proposed model (with attention)	**97.23**

confusion matrix is formed based on actual values according to the dataset and predicted values which are classified by model. It consists of four boxes such as TP, TN, FP, and FN. In this experiment, we have used only diseased images for the comparison with existing models i.e. 613. Therefore, these test images include three types of diseases, i.e., 142 for Meningioma, 186 for Pituitary, and 285 for Glioma. The comparison has been performed with existing models i.e. ResNet50, VGG16, and VGG19.

The detailed results in terms of accuracy, model parameter, and execution time are reported in Table 5. It can be seen that among 142 Meningioma class images, only 2 are incorrectly classified by our proposed model. Moreover, for the Pituitary class, all 186 images are correctly classified and only 2 images of the Glioma class are incorrectly classified by our proposed model. Whereas, ResNet50 incorrectly classified 19 images of Meningioma, 1 of Pituitary, and 19 of Glioma. VGG16 incorrectly classified 28 images of Meningioma, 1 of Pituitary, and 14 of Glioma. Furthermore, VGG19 incorrectly classified 28 images of Meningioma, 1 of Pituitary, and 11 of Glioma. It is depicted from the results that our proposed algorithm achieves 99.5% accuracy on this test data which is the highest accuracy among all along with 99% precision, recall, and F1 score. While second highest accuracy is achieved by ResNet50 i.e. 94.2%. While VGG16 and VGG19 achieved 93.1% and 93.8% accuracy respectively as shown in Fig. 9.

The results of the complete experiment are reported in confusion matrices using 711 test images i.e. 613 diseased images and 98 healthy images from the Kaggle dataset in Fig. 10. In part a, the multi-class classification results are shown. It can be seen that among 98 healthy images, only 2 images are incorrectly classified and among 613 tumorous images, only 4 images have been incorrectly classified. In part b, overall classification results are reported. Therefore, it is worth mentioning that our proposed algorithm performs significantly over test images.

It can be seen from Table 5 that the base frameworks such as VGG16, and VGG19 have high execution time and require large computation resources. Moreover, because these models have a large number of parameters, they take longer to train and, as a result, require more data to effectively learn discriminative properties from input samples to discriminate tumor areas from healthy brain cells. Additionally, these models have a long execution time which makes them unsuitable for real-world applications. While in comparison, the ResNet34-based proposed method is the most robust having fewer model parameters and takes only 1193 seconds to process the input image. The reason for the efficient performance is the network converges quicker and learns the representative features more efficiently by combining different features to reduce redundant computation. On the other hand, the comparative model ResNet50 is more prone to overfitting and has a large computation time as compared to ResNet34. Based on the results, we can conclude that the suggested custom CenterNet with ResNet34 overcomes the shortcomings of comparative approaches and achieves improved performance in terms of classification and computation time complexity.

4.5. Comparative analysis with existing techniques

Here, we discussed the existing techniques based on brain disease detection and classification. We experimented to compare our proposed algorithm with these techniques based on the accuracy. The summary of the results is presented in Table 6. It can be seen that our proposed model based on attention block outperforms the existing ML and DL-based techniques. Whereas, the proposed algorithm without attention block gives an accuracy of 93%, and with attention block attained the accuracy of 98.98% Whereas, the second-highest accuracy is achieved by [27] i.e. 98%. Furthermore, through the experiment, it is depicted that our proposed algorithm is better in computation, feature extraction, and parameter optimization. The comparison graph is shown in Fig. 11.

5. Conclusion

A novel and robust framework for brain tumor detection and classification is presented in this study. We proposed Custom CenterNet in conjunction with the base network, ResNet34 with attention block. ResNet34 with attention block extracts meaningful features from input brain images. Furthermore, these key features were used to train our proposed classifier to detect and classify various types of brain tumors, including Meningioma, Pituitary, and Glioma. Our proposed algorithm can detect brain tumors efficiently in the presence of various artifacts, such as brain shape, size, and orientation of brain images. MRI Brain Scans were used to assess the performance of our proposed system, and various experiments were carried out. The existing deep learning architectures such as ResNet50, VGG16, and VGG19 have been compared with our proposed model using 613 brain test images. Our algorithm achieved 99.3% accuracy on these test images and 98.98% accuracy overall. The proposed method is computationally efficient and fast, as it predicts the tumor's location, size, and class simultaneously. In the future, we plan to extend the proposed approach to predict additional characteristics, such as differentiating benign from malignant tumors and extracting precise tumor areas from localized tumor regions which will aid in better surgical treatment planning. Furthermore, we will consider other databases with different

Table 5
Comparative analysis with DL models based on confusion matrices.

Model	Class	Meningioma	Pituitary	Glioma	Accuracy (%)	Precision (%)	Recall (%)	F1 Score (%)	Parameters (Million)	Execution time (s)
VGG16	Meningioma	114	3	25	93.1	93	93	93	138	2169
	Pituitary	0	185	1						
	Glioma	13	1	271						
VGG19	Meningioma	114	7	21	93.8	91	93	94	143	2217
	Pituitary	0	185	1						
	Glioma	11	0	274						
ResNet50	Meningioma	123	7	12	93.6	93	92	93	23.72	1512
	Pituitary	1	185	0						
	Glioma	16	3	266						
The Proposed Model	**Meningioma**	**140**	**1**	**1**	**99.3**	**99**	**99**	99	**21.5**	**1193**
	Pituitary	**0**	**186**	**0**						
	Glioma	**1**	**1**	**283**						

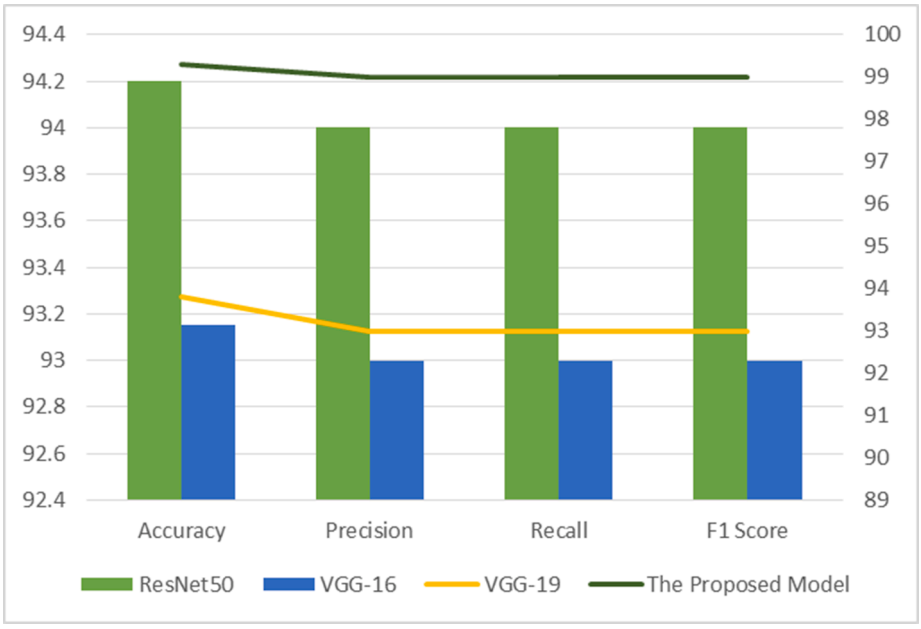

Fig. 9. Comparison with existing DL models for brain tumor detection.

Fig. 10. Confusion matrices for the proposed system over 711 test images.

Table 6
Comparative analysis with existing techniques.

Reference	Year	Algorithm	Accuracy (%)
Sultan et al. [26]	2019	Deep NN	96.13
Deepak et al. [27]	2019	CNN+SVM	98
Çinar et al. [14]	2020	Improved Model	97.01
Saxena et al. [17]	2021	ResNet50	95
Deepak et al. [18]	2021	Custom CNN	95.82
Kibriya et al. [19]	2022	Custom CNN	97.2
Ahuja et al. [4]	2022	DarkNet model	98.54
Proposed Model (without attention)	-	CenterNet+ResNet34	93
Proposed Model (with attention)	-	CenterNet+ResNet34+attention	98.98

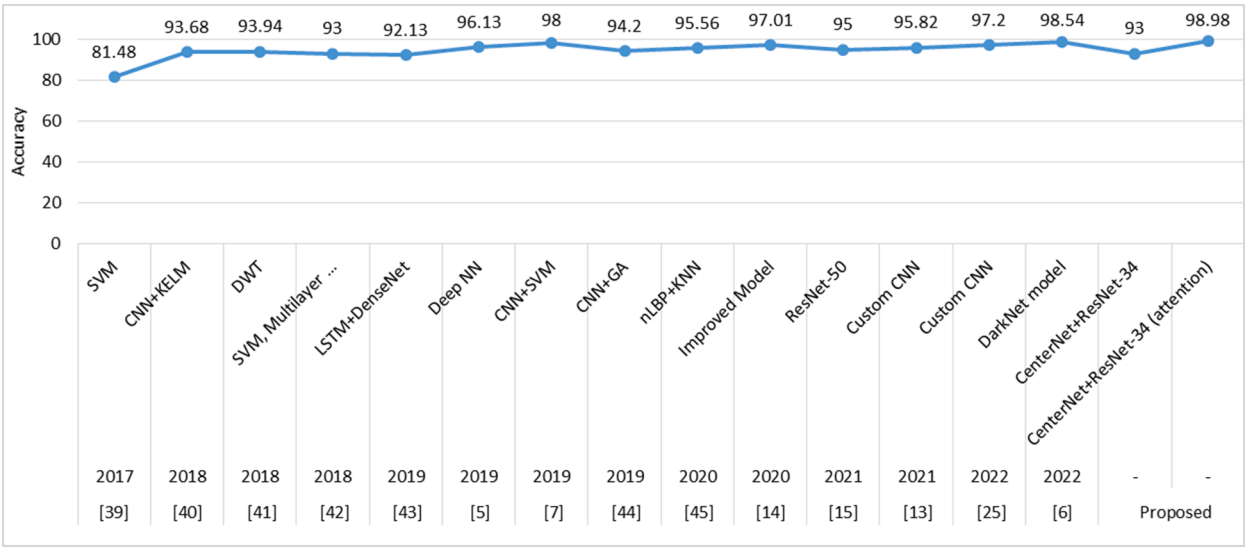

Fig. 11. Comparative analysis with existing techniques.

imaging modalities to learn domain-invariant feature representation in order to improve the generalization capabilities of the proposed model. We further intend to investigate the visualization approaches to qualitatively comprehend the impact of dataset-specific bias on brain tumor classification prediction using the proposed method.

Declaration of Competing Interest

All authors declared that they have no conflict of interest in this study. Thank you

Data availability

Data will be made available on request.

References

[1] Joyia GJ, Liaqat RM, Farooq A, Rehman S. Internet of medical things (IoMT): applications, benefits and future challenges in healthcare domain. J Commun 2017;12:240–7.
[2] Bolhasani H, Mohseni M, Rahmani AM. Deep learning applications for IoT in health care: a systematic review. Inform Med Unlocked 2021:100550.
[3] Masood M, Nazir T, Nawaz M, Mehmood A, Rashid J, Kwon HY, et al. A novel deep learning method for recognition and classification of brain tumors from MRI images. Diagnostics 2021;11:744.
[4] Ahuja S, Panigrahi BK, Gandhi TK. Enhanced performance of dark-nets for brain tumor classification and segmentation using colormap-based superpixel techniques. Mach Learn Appl 2022;7:100212.
[5] Toğaçar M, Cömert Z, Ergen B. Classification of brain MRI using hyper column technique with convolutional neural network and feature selection method. Expert Syst Appl 2020;149:113274.
[6] Swati ZNK, Zhao Q, Kabir M, Ali F, Ali Z, Ahmed S, et al. Brain tumor classification for MR images using transfer learning and fine-tuning. Comput Med Imaging Graph 2019;75:34–46.
[7] Duan K, Bai S, Xie L, Qi H, Huang Q, Tian Q. Centernet: keypoint triplets for object detection. In: Proceedings of the IEEE/CVF international conference on computer vision; 2019. p. 6569–78.
[8] Woo S, Park J, Lee JY, Kweon IS. Cbam: Convolutional block attention module. In: Proceedings of the European conference on computer vision (ECCV); 2018. p. 3–19.
[9] He K, Zhang X, Ren S, Sun J. Deep residual learning for image recognition. In: Proceedings of the IEEE conference on computer vision and pattern recognition; 2016. p. 770–8.
[10] Kalaiselvi T, Padmapriya S, Sriramakrishnan P, Somasundaram K. Deriving tumor detection models using convolutional neural networks from MRI of human brain scans. Int J Inf Technol 2020:1–6.
[11] Dong S, Wang P, Abbas K. A survey on deep learning and its applications. Comput Sci Rev 2021;40:100379.
[12] Kurup RV, Sowmya V, Soman K. Effect of data pre-processing on brain tumor classification using capsulenet. In: Proceedings of the international conference on intelligent computing and communication technologies; 2019. p. 110–9.
[13] Raja PS. Brain tumor classification using a hybrid deep autoencoder with Bayesian fuzzy clustering-based segmentation approach. Biocybern Biomed Eng 2020; 40:440–53.
[14] Çinar A, Yildirim M. Detection of tumors on brain MRI images using the hybrid convolutional neural network architecture. Med Hypotheses 2020;139:109684.
[15] Toğaçar M, Ergen B, Cömert Z. BrainMRNet: brain tumor detection using magnetic resonance images with a novel convolutional neural network model. Med Hypotheses 2020;134:109531.
[16] Ghassemi N, Shoeibi A, Rouhani M. Deep neural network with generative adversarial networks pre-training for brain tumor classification based on MR images. Biomed Signal Process Control 2020;57:101678.

[17] Saxena P, Maheshwari A, Maheshwari S. Predictive modeling of brain tumor: a deep learning approach. Innovations in computational intelligence and computer vision. Springer; 2021. p. 275–85. ed.
[18] Deepak S, Ameer P. Automated categorization of brain tumor from MRI using CNN features and SVM. J Ambient Intell Humaniz Comput 2021;12:8357–69.
[19] Kibriya H, Masood M, Nawaz M, Nazir T. Multiclass classification of brain tumors using a novel CNN architecture. Multimed Tools Appl 2022:1–17.
[20] Aurna NF, Yousuf MA, Taher KA, Azad A, Moni MA. A classification of MRI brain tumor based on two stage feature level ensemble of deep CNN models. Comput Biol Med 2022:105539.
[21] Anilkumar B, Kumar PR. Tumor classification using block wise fine tuning and transfer learning of deep neural network and KNN classifier on MR brain images. Int J Emerg Trends Eng Res 2020;8:574–83.
[22] El Boustani A, Aatila M, El Bachari E, El Oirrak A. MRI brain images classification using convolutional neural networks. In: Proceedings of the *international conference on advanced intelligent systems for sustainable development*; 2019. p. 308–20.
[23] Liu D, Liu Y, Dong L. G-ResNet: improved ResNet for brain tumor classification. In: Proceedings of the *international conference on neural information Processing*; 2019. p. 535–45.
[24] Amin J, Sharif M, Yasmin M, Saba T, Anjum MA, Fernandes SL. A new approach for brain tumor segmentation and classification based on score level fusion using transfer learning. J Med Syst 2019;43:1–16.
[25] Abiwinanda N, Hanif M, Hesaputra ST, Handayani A, Mengko TR. Brain tumor classification using convolutional neural network. In: Proceedings of the *world congress on medical physics and biomedical engineering*; 2018. p. 183–9. 2019.
[26] Sultan HH, Salem NM, Al-Atabany W. Multi-classification of brain tumor images using deep neural network. IEEE Access 2019;7:69215–25.
[27] Deepak S, Ameer P. Brain tumor classification using deep CNN features via transfer learning. Comput Biol Med 2019;111:103345.
[28] Montalbo FJP. A computer-aided diagnosis of brain tumors using a fine-tuned YOLO-based model with transfer learning. KSII Trans Internet Inf Syst 2020;14.
[29] Kaldera H, Gunasekara SR, Dissanayake MB. Brain tumor classification and segmentation using faster R-CNN. Presented at the 2019. In: Proceedings of the advances in science and engineering technology international conferences (ASET); 2019.
[30] Krol A, Gimi B. Medical Imaging 2017: Biomedical Applications in Molecular, Structural, and Functional Imaging. 10137. Society of Photo-Optical Instrumentation Engineers (SPIE) Conference Series; 2017.

Momina Masood received her BS, and MS degrees in Computer Science from Fatima Jinnah Women University Rawalpindi, Pakistan, and the University of Engineering and Technology Taxila Pakistan, respectively. Currently, she is pursuing her Ph.D. in Computer Science at the University of Engineering and Technology Taxila. Her research interests include computer vision, medical image processing, multimedia forensics, and machine learning.

Rabbia Mahum has completed MS in Computer Science from the University of Engineering and Technology, Taxila. Currently, she is serving as Lecturer in Computer Science Department, UET, Taxila. Besides this, she is pursuing PhD from UET, Taxila. Her research areas include Deep learning, Medical image processing, and Video summarization.

Ali Javed is currently working as an Associate Professor in the Department of Software Engineering at UET Taxila Pakistan. He has served as a Postdoctoral Scholar in SMILES lab at Oakland University, USA in 2019 and visiting PhD scholar in ISSF Lab at University of Michigan, USA in 2015. His areas of interest are Computer vision and Video Content Analysis.

Usman Tariq received the Ph.D. degree in information and communication technology in computer science from Ajou University, South Korea. He is experienced in managing and developing projects from conception to completion. He is also attached to the College of Computer Engineering and Science, Prince Sattam bin Abdul-Aziz University.

Muhammad Attique Khan earned his Master and Ph.D degree from COMSATS University Islamabad, Pakistan. He is currently assistant professor of Computer Science Department in HITEC University Taxila, Pakistan. His primary research focus in recent years is medical imaging, Video Surveillance, and Agriculture Plants using Deep Learning. He has above 210 publications that have more than 6000+ citations with h-index 50.

Seifedine Kadry received the bachelor's degree from Lebanese University, in 1999, the M.S. degree from the University of Reims, France, in 2002, and the EPFL, Lausanne, the Ph.D. degree from Blaise Pascal University, France, in 2007, and the H.D.R. degree from the University of Rouen Normandy, in 2017. He is currently a Full Professor with Noroff University College, Norway.